



Published in final edited form as:

Spine (Phila Pa 1976). 2011 September 1; 36(19): 1519–1527. doi:10.1097/BRS.0b013e3181f60b39.

Histological Features of the Degenerating Intervertebral Disc in a Goat Disc-injury Model

YeJia Zhang, M.D., Ph.D.^{*,§,Δ}, Susan Drapeau, Ph.D.[◇], Howard S. An, M.D.[§], Dessislava Markova, Ph.D.[†], Brett A. Lenart, M.D.[§], and D. Greg Anderson, M.D.[†]

^{*} Department of Rehabilitation Medicine, Thomas Jefferson University, Philadelphia, PA

[†] Department of Orthopedic Surgery, Thomas Jefferson University, Philadelphia, PA

[◇] Medtronic Spinal Biologics, Memphis, TN

[§] Department of Orthopedic Surgery, Rush University Medical Center, Chicago, IL

^Δ Department of Physical Medicine & Rehabilitation, Rush University Medical Center, Chicago, IL

Abstract

Study Design—An in vivo study to develop a goat large-animal model for intervertebral disc (IVD) degeneration.

Objectives—To determine an optimal method for inducing goat IVD degeneration suitable for testing disc regeneration therapies.

Summary of Background Data—Although rodent, rabbit, and other small animal studies are useful, the narrow dimensions of IVDs in these species limit studies requiring injection of a relevant volume of therapeutics or implantation of engineered tissue constructs. For this study, the goat was selected because the size and shape of their IVDs are comparable to those of adult humans.

Methods—A minimally invasive approach that did not cause significant morbidity or mortality to adult goats ($n = 6$) was used. Under fluoroscopic guidance, goat lumbar IVDs were injured with a 4.5 mm drill bit or #15 or #10 surgical blades. Two months post-injury, the goats were euthanized and their IVDs with adjacent endplates were isolated, decalcified and stained.

Results—A numerical histological scale to categorize the degree of goat IVD degeneration was developed based on the histological features of rabbit IVDs previously described by Masuda et al., goat IVDs described by Hoogendoorn et al., and human IVDs described by Boos et al. The inter-rater agreement of our scoring system was assessed (weighted Kappa value = 0.6646). Mann-Whitney tests were used to compare the injured IVDs with uninjured control. A 4.5 mm drill bit inserted to a 15 mm depth resulted in a significantly higher histological score compared to uninjured controls ($p = 0.01$). Injury with a #15 or #10 blade did not result in increased histological scores compared with uninjured controls.

Conclusions—A comparison of the various injuries inflicted showed that the use of a 4.5 mm drill bit resulted in the most significant histological changes.

INTRODUCTION

Degenerative disc disease with its associated back pain is a prevalent problem in our aging human population.¹ To study the treatment of degenerative disc disease, large animal models are needed. To date, much of the basic science work related to disc regeneration therapies has been done in small animals, often in rabbits or rodents. While these small animal studies are useful for laying some of the groundwork for human clinical studies, the

narrow dimensions of the intervertebral disc (IVD) in these species limit the ability to study regeneration strategies requiring the injection of a volume of a therapeutic agent relevant to humans, the implantation of tissue-engineered constructs, or the testing of human devices. To develop a useful large animal model, a reliable method of creating disc degeneration and a histological scale to categorize the degree of IVD degeneration in response to injury are required. The optimal method would allow researchers to establish moderate to severe degeneration of the IVD over a relatively short time using a minimally invasive approach that does not cause significant morbidity or mortality to the animals. We developed a fluoroscopically-guided direct lateral approach to injure the goat IVD. This method allows access to the lateral aspect of the disc with minimal morbidity to the research animals. Our study sought to establish a disc injury method capable of creating reproducible degeneration in a time frame that allows the expeditious conduct of research protocols.

The rationale for the use of the goat as a large animal IVD degeneration model is twofold. First, goat discs have anatomic dimensions and shapes similar to those of adult human discs. Second, the use of the goat is pragmatic. The species is hardy and tolerates surgery well, is relatively economical to work with, and is readily available at many animal research facilities. Other large animal models for IVD degeneration have been previously described, including porcine,²⁻⁵ ovine⁶⁻¹¹ and canine¹²⁻¹⁴ models. While each of these models has certain strengths, each also has limitations, including species-specific anatomic variations, a lack of ready availability, concerns related to perioperative morbidity, and ethical concerns regarding their usage.

A porcine model using anular laceration⁵ or endplate injury²⁻⁴ has been described. However, the large size to which pigs grow over several months of follow up make it difficult to use this animal model for longer term studies. The ovine model, which is based on an anular injury, has also been widely used since the 1990s.⁶⁻¹¹ However, there are significant anatomic differences between the size and shape of sheep and human discs that limit the use of this model for tissue engineering studies.¹⁵ The goat seemed to be a more appropriate model, especially for testing of engineered or artificial tissues where migration of the implants could result in serious consequences clinically.¹⁶ Canine models have also been used to study disc degeneration and cell injection therapies.^{12-14,17} However, discs from purpose-bred dogs are significantly smaller than human discs. Additionally, the use of dogs in research has led to significantly increased regulations and ethical scrutiny in some regions of the world.

Goats have been previously used in disc research. Hoogendoorn et al. studied goat disc degeneration using chondroitinase ABC digestion.^{18,19} They found slow, progressive degeneration of IVDs induced by intradiscal injection of 0.25 unit/ml of chondroitinase ABC.¹⁸

Although the goat has many advantages for studying disc tissue engineering in a larger animal model, certain other aspects of this goat model required investigation. A reliable technique to produce an anular injury in the goat had not yet been established, and a histological grading scheme for the ensuing degeneration needed to be described and validated. Therefore, in the current study, we aimed to establish an optimal anular injury technique in goat discs that would lead to reliable degeneration, and to describe and validate a numeric histological scoring system with which to quantify the degree of IVD degeneration.

The goat model has several other advantages. The goats we used weighed about 180 pounds, similar to that of an adult human. These goats tolerated general anesthesia well and there was no death among our animals due to anesthesia accidents or infection. The trunk of the

goat is relatively small in width, facilitating lateral access to the disc. Using tubular retractors designed for minimally invasive lumbar surgery, the disc can easily be reached from a direct lateral approach, allowing therapeutic interventions with minimal operative site morbidity. Finally, goat lumbar disc heights are only slightly less than those of humans, and the adequate anteroposterior and medial to lateral dimensions would allow “human-sized” implants or constructs to be used. This feasibility study aimed to establish an injury-induced model of disc degeneration, one that more closely mimics human disc degeneration subsequent to an annular tear.

METHODS

Surgical Techniques

The instruments used to induce injury and sample X-rays obtained during surgery were illustrated in Figure 1. Six male Nubian goats approximately four years of age were used. The Nubian goats are sexually mature as early as 6 months old. Their normal life span is 8–12 years. The four-year-old goats used here are considered skeletally mature, comparable to young adult humans, and their IVDs are free of notochordal cells.²⁰ Sexually mature goat still has growth plates, which suggest that the animal may still have growth capacity. In comparison, adult human vertebral body does not contain secondary apophyseal centers. The use of these animals was approved by the Institutional Animal Care and Use Committee (IACUC) of Thomas D. Morris, Inc. (Reisterstown, MD; #06-052). Under general anesthesia, the goats were positioned in the lateral decubitus position with the right side up. The skin was shaved and prepared for sterile procedures. Lateral X-ray images were obtained using a C-arm fluoroscopic imager. First, a small ~14 mm skin incision was made directly at a site over the mid-lateral aspect of the disc as determined by the C-arm. Next, a small, blunt dilator (METRx Microdiscectomy System, Medtronic Sofamor Danek, Memphis, TN) was gently passed through the skin incision, in line with the fluoroscopic beam, until the lateral surface of the anulus was palpated. Sequentially larger dilators were placed over the initial dilator until a 14 mm tubular retractor could be inserted through the opening (Figure 1B). Figure 1A shows instruments used to create injuries. Working through the tubular retractor under fluoroscopic guidance, T13/L1, L1/2, L2/3, and L3/4 spinal levels were approached. The discs were randomly assigned as the site of the following injuries: 1) a #10 blade inserted parallel to the endplate to the depth of the blade attachment (Figure 1C); 2) a #15 blade inserted twice, first parallel to the endplate, to the depth of the blade attachment, and second vertically to the endplate (in cruciate fashion); 3) a drill bit 4.5 mm in diameter, inserted 15 mm and rotated manually 360 degrees (Figure 1D). Lateral fluoroscopic images were recorded intra-operatively to verify placement of the instruments. L4/5 and L5/6 discs were reserved as uninjured controls.

Following the creation of a disc annular lesion, the tubular retractor was withdrawn and the wounds were irrigated and closed with staples. The animals were allowed to recover from anesthesia and then returned to their normal living quarters. They were fed normal goat chow and allowed to carry out normal activity without restriction.

Two months following injury, lateral X-rays and MRI images of discs were obtained under general anesthesia. The goats were then euthanized with an overdose of pentobarbital, and their spines were harvested en-block for analysis.

Tissue Preparation

The intervertebral discs with approximately 1/3 of the adjacent bony vertebral body were isolated at each level. The bone-disc-bone segments were then transected sagittally with a band saw. Since the injury was induced using an anterior-lateral approach, crossing the

midline. Sagittal sections at midline allow us to consistently include the injured part in our histological analysis. Gross pictures were taken with a digital camera (shown in Figure 6 below).

Tissue Preparation for Histology

Immediately after dissection, the disc with its surrounding endplates was fixed in 10% formaldehyde for one week. Subsequently, the soft tissues were further trimmed closer to the endplate, keeping the endplate intact. The disc-endplate segments were decalcified using 12.5% EDTA at pH 7.8 with daily solution changes for about four months, until the bone was completely decalcified.

The tissues were embedded in paraffin, sectioned to 5 μm thickness, and stained with Alcian blue, using Haematoxylin and Eosin (H&E) as a counter stain. To better visualize cell morphology, adjacent sections were stained using H&E alone. Tissue sections were deparaffinized, stained with 1% Alcian blue Solution (Poly Scientific R&D Corp., Bay Shore, N.Y.) for 5 minutes, and then stained with Haematoxylin for 5 minutes and Eosin for 20 seconds.

Histological Evaluations

A modified histological grading scale for large animal discs based on prior work of Masuda et al.²¹, Hoogendoorn et al.,¹⁸ and Boos et al.²² was developed. As shown in Table 1, a numeric scale for quantification of the degree of degeneration was designed. Analysis included the status of the following four categories: i) integrity of the border between the nucleus pulposus (NP) and the anulus fibrosus (AF); ii) AF organization; iii) the status of the extracellular matrix in the NP; iv) cellularity of the NP. Total scores ranged from 0 to 8. Scores of 0–2.0 represent essentially normal tissue; IVDs with mild disc degeneration scored 2.1–4.0 points; IVDs with moderate degeneration scored 4.1–6.0; IVDs with severe degeneration scored 6.1–8.0. Histological sections were imaged using a Nikon Eclipse microscope and Nikon NIS-Elements software (Melville, NY, USA).

Detailed descriptions of each category in the grading scheme follow:

I. Anulus fibrosus (AF) and nucleus pulposus (NP) border—The integrity of the AF and NP border was determined using low magnification (1X and 4X). Figure 2 shows IVD tissue sections stained with H&E (panels A, B, and C) or Alcian blue with H&E counter staining (panels D, E, and F), and photographed using a low (1X) magnification lens. A distinct transition from AF to NP was considered “a normal border” (panels A and D), and given a score of 0. Tissues with a minimally interrupted transition between AF and NP (panels B and E) were given a score of 1. This was characterized as a gradual blurring of the transition from NP to AF, frequently with thinning of the AF, especially the posterior portion of the AF. Note that arrows point to the posterior AF. Tissues with severe loss of a distinguishable transition from NP to AF (panels C and F) were given a score of 2.

II. Anulus Fibrosus (AF) Organization—The AF organization was determined using low magnification (4X). Figure 3 shows IVD tissue sections stained with Alcian blue with H&E counter staining, and examined under 4X magnification. Tissues with normal lamellar organization (panel A) were given a score of 0. Sections with slightly disorganized anular rings (panel B) were given a score of 1. Note that the arrow points to disorganized anular fibers. Tissues with gross loss of lamellar organization were given a score of 2.

III. Extracellular matrix of the nucleus pulposus (NP)—The degree of NP matrix condensation was determined using 10X magnification. Figure 4 illustrates the extracellular

matrix appearance of normal and degenerative NP tissues. The sections were stained with Alcian blue, and examined using 10X magnification. Panel A shows NP tissue with a normal gelatinous appearance, given a score of 0. In Panel B, NP tissues show mild condensation of the extracellular matrix, given a score of 1. Panel C shows NP tissues with a severely condensed extracellular matrix, assigned a score of 2. Panel D illustrates matrix lagoons around chondrocyte islands, indicating that these chondrocytes were producing large amounts of secreted matrix material; these were also given a score of 1.

IV. Nucleus Pulposus (NP) cellularity and cell morphology—Sections stained with Alcian blue with H&E counter staining were examined under high magnification (10X and 20X). Figure 5 illustrates NP tissues examined and scored for cellularity. Panel A shows normal cellularity with chondrocyte-like cells, resulting in a score of 0. Panel B shows a moderate degree of cell density increase in NP tissues (arrow points to a fibrocyte-like cell); these tissues were given a score of 1. Severe changes in cell density (both hypo-cellular and hypercellular) were assigned a score of 2. Panel C shows a severe decrease in cell density (hypocellular, the small arrow points to a fibrocyte-like cell); this tissue was given a score of 2. Panel D shows a region within the NP tissue that is hypercellular with chondrocyte cloning (the large arrow indicates a cluster of cells); these tissues were also assigned a score of 2. Cell morphology changes such as cell cloning (clusters of cells shown in Panel D) or transitions into fibrocyte-like cells (Panel B & C) were noted, but were not included in the scores.

Upon completion of the histological scoring, the sum of the histological scores derived from the four categories described above was obtained. Scores for severity of the injury were grouped according to total scores (Table 2).

Magnetic Resonance (MR) Imaging

MR images of the goat lumbar spine were obtained using a 1.5 Tesla clinical imager before disc injury, with the animals under general anesthesia. MR images of the same resolution were also obtained on lumbar spines isolated en-block immediately after sacrifice.

Statistical Methods

The sum of the four histological criteria was calculated. Inter-observer variability was assessed by a weighted Kappa using SAS software.²³ Histological scores of discs injured by the three different methods were compared with those of uninjured controls. Mann-Whitney test was used to calculate p-values. The confidence interval was 95%.

RESULTS

Gross Morphology

In a previous experiment, a size #15 blade scalpel was inserted once, parallel to the endplate but failed to induce detectable histological degeneration at the three-month and six-month time points (data not shown). In the current study, in order to produce a more severe injury to the IVD that would lead to reliable progressive degeneration, other injury methods were tested including: **1**) a #15 blade inserted parallel to the endplate, to depth of the blade attachment, followed by 90 degree insertion of the blade to the blade attachment perpendicular to the endplate (**cruciate injury**); **2**) a #10 blade inserted parallel to the endplate to the depth of the blade attachment; **3**) a 4.5 mm diameter drill bit inserted to a depth of 15 mm and then rotated 360 degrees within the disc. Figure 6 shows the gross morphology of discs. **Panel A** is a photo of an uninjured disc with a normal, gel-like NP that bulges upon slicing in the sagittal plane. The concentric rings of the AF are evident. The border between the NP and AF is clear. **Panel B** shows a disc that received a cruciate injury

with a #15 blade. **Panel C** is a disc injured with a #10 blade. The NP did not bulge and appeared dull and rubbery. The anular rings are not easily visible with the naked eye and the margins of the NP and AF are blurred. **Panel D** is a photo of a disc injured with a drill bit 4.5 mm in diameter, inserted 15 mm into the disc, and rotated 360 degrees within the disc. The NP had lost its shiny appearance and did not bulge upon sagittal sectioning. The AF rings are not visible, and the NP-AF border is not distinguishable. Note that disc heights increase as one moves more caudally in the spine, therefore we were not able to compare disc height among the treatment groups because the levels were randomized to injury treatment.

Comparison of Histological Scores between Treatment Groups

Two evaluators, one board certified physician specializing in rehabilitation and one a basic science researcher specializing in hard tissue morphology, evaluated the tissues. The sum of the scores from each of the four categories was calculated, and average scores for control and treatment categories were compared (Table 2). Inter-reader variability of the total histological score was analyzed as described by Cohen.²⁴ A total histological score difference of one or less was considered an agreement. The agreement between the two readers was 91.4%. The weighted Kappa value was 0.6646, with a 95% confidence interval of 0.5638 to 0.7655. A weighted Kappa value of 0.6646 indicates that there is substantial, although not perfect, agreement in the histological scores between the two readers. Based on the criteria described above, histological scores were summed and averaged between the two readers (Table 2). The scores between injured discs and uninjured control discs were analyzed using the Mann-Whitney test. Among various injury methods, the 4.5 mm drill bit inserted to a 15 mm depth resulted in the highest histological score, significantly higher than that for the uninjured control ($p = 0.01$). IVDs injured with a #15 blade twice in a cruciate fashion, or a #10 blade inserted once parallel to endplate did not differ significantly in histological scores from uninjured controls (both $p = 0.26$). Note that a combined score of the L4/5 and L5/6 IVDs were used as uninjured controls.

Histological values for the four criteria for the different animals are summarized in Table 3. All four categories appear to have a significant impact on the total histological score.

We suggest that the injury-induced disc degeneration be divided into four levels: 1. normal (histological grade 0–2); 2. Mild degeneration (grade 3–4); 3. Moderate degeneration (grade 5–6); 4. Severe degeneration (grade 7–8). Among the three types of injuries, drill bit resulted in moderate degeneration (mean grade 5.1), #10 blade resulted in mild degeneration (mean grade 3.1), and #15 blade injured discs had a histological score in the normal range (1.8).

MR Imaging of the Spine

The intact animal before IVD injury and the isolated spine blocks immediately following euthanasia were compared using T2 weighted 1.5 Tesla MR images. The images were graded by three independent evaluators according to Pfirrmann et al.²⁵ No significant differences in disc grading by the Pfirrmann classification were found between these two time points.

Discussion

Our data show that a drill bit injury is a reliable method that induced mild to moderate disc degeneration within two months. In addition, the histology scoring correlated with the gross morphology, as documented by photographs shown in Figure 6. Across the spectrum of observed changes, our histological grading system correlated with changes in gross morphology, suggesting the validity of our scoring system. Additional study of biochemical

parameters (e.g., proteoglycan and collagen contents) is indicated. This line of study will be especially useful to determine whether quantitative characterization of the histological changes correlates with biochemical changes, further validating our histological grading scheme.

We have observed spontaneous mild degeneration of the two uninjured caudal lumbar discs (L4/5 and L5/6 discs). Most goats have a total of six lumbar vertebrae with L6 located immediately cranial to the sacrum. The Nubian goat has an average lifespan of 12 years. Therefore, the four year old goats used in this study were approximately 25% through their life spans, equivalent to a young adult human. It is not entirely surprising that the L4/5 and L5/6 IVDs show mild spontaneous degenerative changes. Similarly, in humans, these lower two lumbar discs are the most prone to natural degeneration, presumably for biomechanical reasons. Therefore, these two levels do not serve as an optimal “normal” control in this model. Alternatively, the experiment could have been designed such that the uninjured controls were randomized in the same way as the various injured levels. However, this would result in uninjured control levels “sandwiched” between two injured levels, and would raise concerns over accelerated degeneration adjacent to degenerative areas, and thus less mobile motion segments. Finally, other goats with sham surgeries could be used as controls, but individual variability and increased cost would be a concern.

Several other methods to induce IVD degeneration have been reported. Hoogendoorn et al. also found the goat to be a suitable model for studying disc degeneration caused by digestion with chondroitinase ABC.^{18,19} This enzyme degrades chondroitin sulfate chains with great specificity. This enzymatic technique for inducing degeneration was also used by others in small animals, such as rabbits, and *in vitro* by Ando et al.²⁶ It has been hypothesized that limited proteolysis in the anulus induces a dramatic decrease in the ability of the disc to undergo reversible deformation with destabilization of the collagen network. Our previous experience with rabbits produced more rapid and less controllable degeneration with enzymatic digestion compared to needle puncture (data not shown). However, in the goat, which appears more prone to slower degeneration after annular injury, a direct comparison of enzymatic digestion to annular injury is warranted to define the optimal model of producing an injury that would permit the study of tissue engineering techniques. Disc degeneration induced by nucleotomy using a suction device has been described by Nguyen et al., and may provide a method for inducing more severe disc degeneration.²⁷ However, this method remains to be tested in a goat model, perhaps because the normal goat NP tissue is firm (Figure 6) and may not be prone to herniation. Our observation is that adult human NP is similar in firmness to that of goat. For research scenarios requiring more severe degrees of degeneration, a more severe injury, longer follow up time point, and alternative means of inducing degeneration (nucleotomy or enzymatic digestion) should be considered.

Significant changes in cell density, morphology and matrix appearance were observed in our study. In hypocellular discs, the matrix tended to show more severe condensation with a more fibrocyte-like cell population, perhaps suggesting that discs with changes in cell behavior and number are not able to maintain the disc matrix. Other discs demonstrated hypercellularity with lagoons of extracellular matrix around enlarged cells, more suggestive of an attempted reparative response. In our histological grading system, cell density in the NP has been listed as a separate category, in addition to the AF organization, border between AF and NP, and NP matrix described by Hoogendoorn et al.¹⁸ Changes in cell morphology were described, but were not included in the scores. Our histological scheme comprised four categories, simplified from the 11 category human classification described by Boos et al.²² Compared with human IVD degeneration, the injury-induced degeneration in this study is equivalent to grade II and III according to Thompson et al.²⁸

The goat disc injury model described in our report differs significantly from the sheep model anular injury initially described by Osti et al.^{7,8,29,30} For example, we used a 4.5 mm drill bit inserted to a 15 mm depth, which caused a full thickness injury to the anulus and the nucleus, with the tip of the drill bit approaching the posterior anulus. The sheep anular defect was only 5 mm deep by 5 mm wide, which only disrupts the fibers in the outer third of the anular rim.^{6,7,9} Following this anular rim lesion, the outer anulus undergoes spontaneous repair, but the non-repaired inner anular defect propagates further, resulting in secondary delamellations, circumferential or radial tears, loss of disc height and disc degeneration.¹¹

Surprisingly, MRI grading did not change in a consistent fashion between the pre-injury state and the two month post-injury time point. This may be due to the relatively mild degenerative changes induced in this model. Future studies using higher resolution MR imaging techniques, and “MRI” index as described by Sobajima *et al.* may produce better results.³¹

The current study has a number of limitations which must be acknowledged. One disadvantage of the current model includes one present in all large animal models: a relatively long time for degeneration to occur. Furthermore, the spines of quadrupeds sustain different biomechanical forces from those in humans, who are adapted to an upright posture.³² Although the biomechanics of the goat spine have not been thoroughly elucidated, we expect similarities with other large quadruped animals. Also, specific gene sequences in the goat are at present largely unavailable; thus it is difficult to study gene expression in response to injuries and treatments. Depending on the nature of the study, these disadvantages may be outweighed by the similarities in size and shape of goat IVDs to those of humans, ease of working with this model, and the availability and cost that compare favorably with other large animal models.

Additional limitations of the current goat disc injury model are listed below. First, the number of animals included in the study was small ($n = 6$). Second, the control disc chosen showed histological signs of spontaneous degeneration. Third, only our most severe injury was able to produce significant degeneration by two months post-injury. The lack of more profound histological changes may be due to the relatively short observation period after injury, and remarkable ability of tissue repair by this breed of goat. Fourth, we did not do biochemical analysis of the discs to further quantify the degree of degeneration and validate the histological scoring system. Finally, the routine MRI with 1.5 Tesla resolution failed to produce meaningful data for analysis of degeneration. However, in the development and characterization of a new model, it should be understood that even negative information may prove useful to other researchers interested in using a large animal model for disc research. Future directions include a longer time course, biochemical analysis, and high resolution MR imaging studies.

We have developed a minimally invasive approach to access the goat IVD, a drill bit injury method for inducing disc injury, and a quantitative histological injury scale. These new methods should prove useful to researchers wanting to study regeneration strategies that require the injection of a larger volume of therapeutics or the implantation of engineered tissue constructs.

Acknowledgments

Dr. Yejia Zhang was supported by a grant from the Eunice Kennedy Shriver National Institute of Child Health and Human Development (NICHD, 1K08 HD049598-01). The Medtronic Spinal Biologics Company provided funding for the animal work and histological supplies. The authors gratefully acknowledge Dr. Carol Muehleman for critically reviewing the histological score criteria, and scoring the histological sections. The authors thank Dr.

Harvey Smith and Betty Picinic for photographing sections of the IVD tissue, and for valuable discussions regarding histological features related to injury. The authors also gratefully acknowledge Julie Sterman for performing MRI on spines isolated two months after IVD injury, and Dr. Eugene Thonar and Dr. Gunnar Andersson for valuable insights and discussions. We thank Dr. Jorge Roman-Blas, M.D. and Yiding Shen for goat tissue dissections. The authors would also like to thank Dr. Todd Beck and Dr. Kimberly A. Skarupski for inter-observer variability analysis and valuable insights in statistical methods. We gratefully acknowledge Dr. Ana Chee and Christian Park for manuscript preparation.

References

1. United States Bone and Joint Decade: The Burden of Musculoskeletal Diseases in the United States. Rosemont, IL: The American Academy of Orthopaedic Surgeons; 2008.
2. Holm S, Baranto A, Kaigle Holm A, et al. Reactive changes in the adolescent porcine spine with disc degeneration due to endplate injury. *Vet Comp Orthop Traumatol.* 2007; 20:12–7. [PubMed: 17364090]
3. Holm S, Ekstrom L, Kaigle Holm A, et al. Intradiscal pressure in the degenerated porcine intervertebral disc. *Vet Comp Orthop Traumatol.* 2007; 20:29–33. [PubMed: 17364093]
4. Holm S, Holm AK, Ekstrom L, et al. Experimental disc degeneration due to endplate injury. *J Spinal Disord Tech.* 2004; 17:64–71. [PubMed: 14734978]
5. Kaapa E, Holm S, Han X, et al. Collagens in the injured porcine intervertebral disc. *J Orthop Res.* 1994; 12:93–102. [PubMed: 8113947]
6. Melrose J, Ghosh P, Taylor TK, et al. A longitudinal study of the matrix changes induced in the intervertebral disc by surgical damage to the annulus fibrosus. *J Orthop Res.* 1992; 10:665–76. [PubMed: 1500980]
7. Melrose J, Ghosh P, Taylor TK, et al. Elevated synthesis of biglycan and decorin in an ovine annular lesion model of experimental disc degeneration. *Eur Spine J.* 1997; 6:376–84. [PubMed: 9455664]
8. Melrose J, Roberts S, Smith S, et al. Increased nerve and blood vessel ingrowth associated with proteoglycan depletion in an ovine annular lesion model of experimental disc degeneration. *Spine.* 2002; 27:1278–85. [PubMed: 12065974]
9. Melrose J, Smith S, Little CB, et al. Spatial and temporal localization of transforming growth factor-beta, fibroblast growth factor-2, and osteonectin, and identification of cells expressing alpha-smooth muscle actin in the injured annulus fibrosus: implications for extracellular matrix repair. *Spine.* 2002; 27:1756–64. [PubMed: 12195068]
10. Melrose J, Smith S, Little CB, et al. Spatial and temporal localization of transforming growth factor-beta, fibroblast growth factor-2, and osteonectin, and identification of cells expressing alpha-smooth muscle actin in the injured annulus fibrosus: implications for extracellular matrix repair. *Spine (Phila Pa 1976).* 2002; 27:1756–64. [PubMed: 12195068]
11. Melrose J, Smith SM, Little CB, et al. Recent advances in annular pathobiology provide insights into rim-lesion mediated intervertebral disc degeneration and potential new approaches to annular repair strategies. *Eur Spine J.* 2008; 17:1131–48. [PubMed: 18584218]
12. Ganey THW, Moseley T, Hedrick M, Strem B, Meisel HJ. Intervertebral Disc Repair Using Adipose tissue-Derived Stem and Regenerative Cells: Experiments in a Canine Model. *Proceedings for the International Society for the Study of Lumbar Spine.* 2009:67.
13. Ganey TM, Meisel HJ. A potential role for cell-based therapeutics in the treatment of intervertebral disc herniation. *Eur Spine J.* 2002; 11 (Suppl 2):S206–14. [PubMed: 12384746]
14. Hasegawa K, Turner CH, Chen J, et al. Effect of disc lesion on microdamage accumulation in lumbar vertebrae under cyclic compression loading. *Clin Orthop Relat Res.* 1995:190–8. [PubMed: 7634575]
15. Meakin JR, Reid JE, Hukins DW. Replacing the nucleus pulposus of the intervertebral disc. *Clin Biomech (Bristol, Avon).* 2001; 16:560–5.
16. Schnake KJ, Weigert F, Kandziora F, et al. Local vertebral body destruction after migration of a nucleus replacement. *Z Orthop Unfall.* 2007; 145:649–51. [PubMed: 17939078]
17. Ganey T, Libera J, Moos V, et al. Disc chondrocyte transplantation in a canine model: a treatment for degenerated or damaged intervertebral disc. *Spine.* 2003; 28:2609–20. [PubMed: 14652478]

18. Hoogendoorn RJ, Helder MN, Kroeze RJ, et al. Reproducible long-term disc degeneration in a large animal model. *Spine*. 2008; 33:949–54. [PubMed: 18427314]
19. Hoogendoorn RJ, Wuisman PI, Smit TH, et al. Experimental intervertebral disc degeneration induced by chondroitinase ABC in the goat. *Spine*. 2007; 32:1816–25. [PubMed: 17762288]
20. Hoogendoorn RJ, Helder MN, Smit TH, Wuisman PIJM. Notochordal Cells in Mature Caprine Intervertebral Discs. *European Cells and Materials*. 2005; 10(Suppl 3):59.
21. Masuda K, Aota Y, Muehleman C, et al. A novel rabbit model of mild, reproducible disc degeneration by an annulus needle puncture: correlation between the degree of disc injury and radiological and histological appearances of disc degeneration. *Spine*. 2005; 30:5–14. [PubMed: 15626974]
22. Boos N, Weissbach S, Rohrbach H, et al. Classification of age-related changes in lumbar intervertebral discs: 2002 Volvo Award in basic science. *Spine*. 2002; 27:2631–44. [PubMed: 12461389]
23. SAS 9.2 Help and Documentation. Cary, NC: SAS Institute Inc; 2000–2004.
24. Cohen RB. A coefficient of agreement for nominal scales. *Educational and Psychological Measurement*. 1960; 20:37–46.
25. Pfirrmann CW, Metzdorf A, Zanetti M, et al. Magnetic resonance classification of lumbar intervertebral disc degeneration. *Spine*. 2001; 26:1873–8. [PubMed: 11568697]
26. Ando T, Kato F, Mimatsu K, et al. Effects of chondroitinase ABC on degenerative intervertebral discs. *Clin Orthop Relat Res*. 1995:214–21. [PubMed: 7671520]
27. Nguyen CM, Haughton VM, Ho KC, et al. A model for studying intervertebral disc degeneration with magnetic resonance and a nucleotome. *Invest Radiol*. 1989; 24:407–9. [PubMed: 2745024]
28. Thompson JP, Pearce RH, Schechter MT, et al. Preliminary evaluation of a scheme for grading the gross morphology of the human intervertebral disc. *Spine*. 1990; 15:411–5. [PubMed: 2363069]
29. Fazzalari NL, Costi JJ, Hearn TC, et al. Mechanical and pathologic consequences of induced concentric annular tears in an ovine model. *Spine*. 2001; 26:257–81.
30. Osti OL, Vernon-Roberts B, Fraser RD. 1990 Volvo Award in experimental studies. Annulus tears and intervertebral disc degeneration. An experimental study using an animal model. *Spine (Phila Pa 1976)*. 1990; 15:762–7. [PubMed: 2237626]
31. Sobajima S, Kempel JF, Kim JS, et al. A slowly progressive and reproducible animal model of intervertebral disc degeneration characterized by MRI, X-ray, and histology. *Spine*. 2005; 30:15–24. [PubMed: 15626975]
32. Kettler A, Liakos L, Haegeler B, et al. Are the spines of calf, pig and sheep suitable models for pre-clinical implant tests? *Eur Spine J*. 2007; 16:2186–92. [PubMed: 17721711]

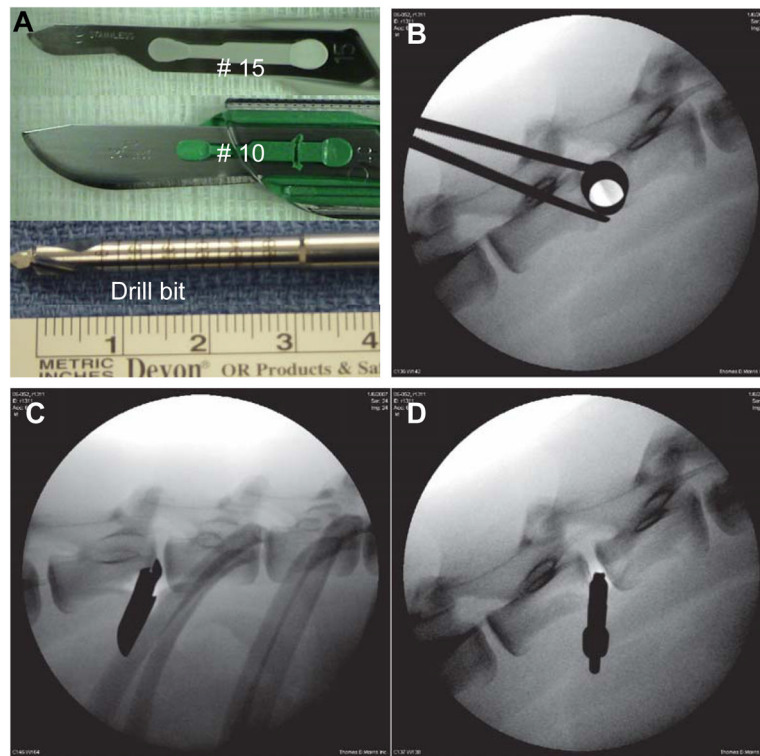


Figure 1. Instruments used to induce disc injury in the goat and sample X-rays obtained during surgery

A. The instruments used to create disc injuries (from top to bottom: #10 blade, #15 blade, 4.5 mm drill bit); **B–D:** lateral X-ray of the goat spine documenting the positions of the instruments: **B.** large dilator inserted adjacent to the intervertebral disc; **C.** the #10 blade; **D.** the 4.5 mm drill bit.

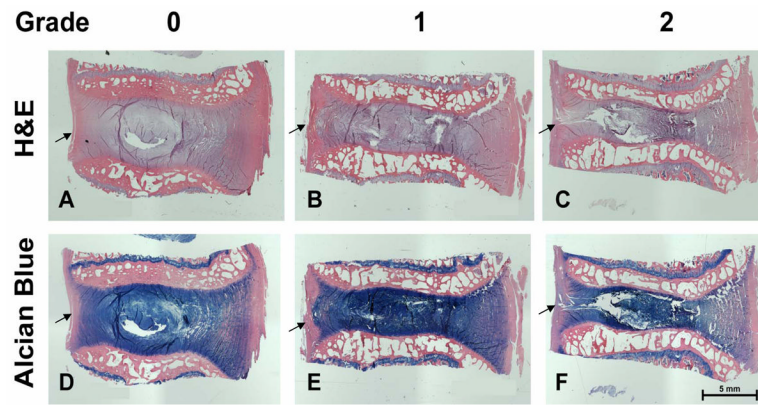


Figure 2. Border between annulus fibrosus (AF) and nucleus pulposus (NP) of the goat intervertebral disc

Sagittal tissue sections were stained with Haematoxylin and Eosin (H&E) (panels A, B, and C) or Alcian blue with H&E counterstaining (panels D, E, and F). Panels A & B: normal border; Panels B & E: minimal blurring of border; C & F: loss of distinguishable border between NP and AF. Arrows point to the posterior AF.

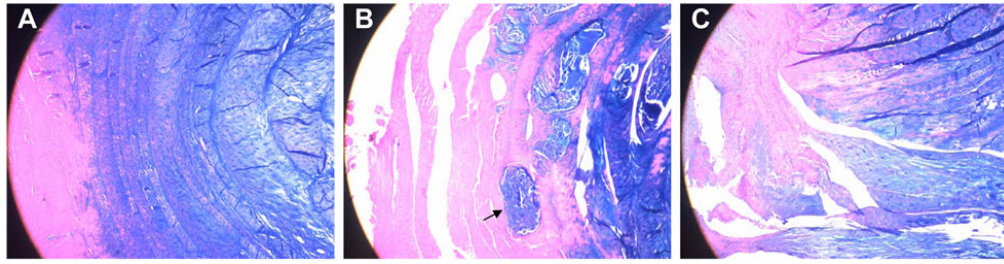


Figure 3. Anulus Fibrosus (AF) Organization of the goat disc
A. normal lamellar organization; **B.** slightly disorganized anular rings (arrow points to disorganized anular fibers); **C.** gross loss of lamellar organization.

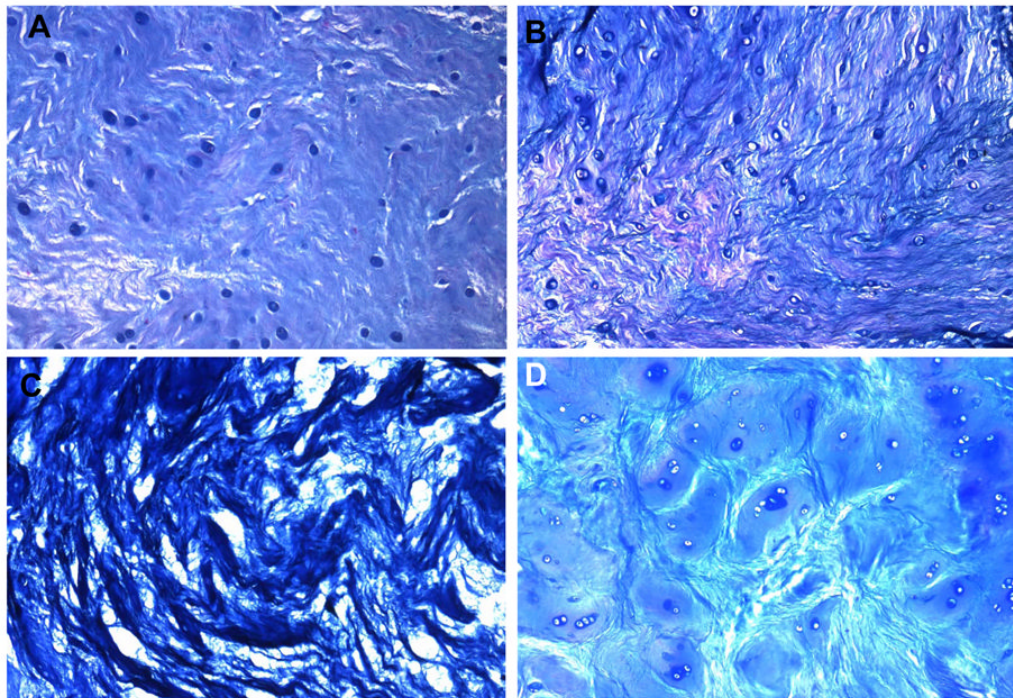


Figure 4. Extracellular matrix of the nucleus pulposus (NP) of the goat disc
NP tissues were stained with Alcian blue. **A.** normal gelatinous appearance; **B.** mild condensation of the extracellular matrix; **C.** severe condensation of the extracellular matrix; **D.** matrix lagoons around chondrocyte islands.

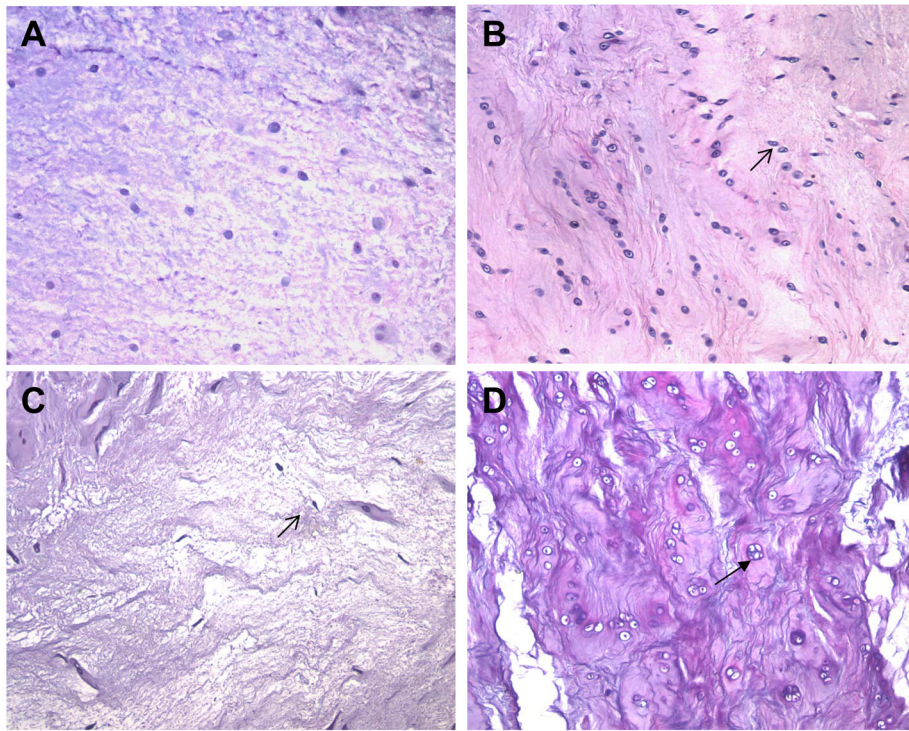


Figure 5. Goat nucleus pulposus (NP) cellularity and cell morphology

A. normal cellularity with chondrocyte-like cells; **B.** hypercellular with fibrocyte-like cells (open arrow points to a fibrocyte-like cell); **C.** hypocellular with fibrocyte-like cells; **D.** hypercellular with chondrocyte cloning (solid arrow indicates a cluster of cells.)

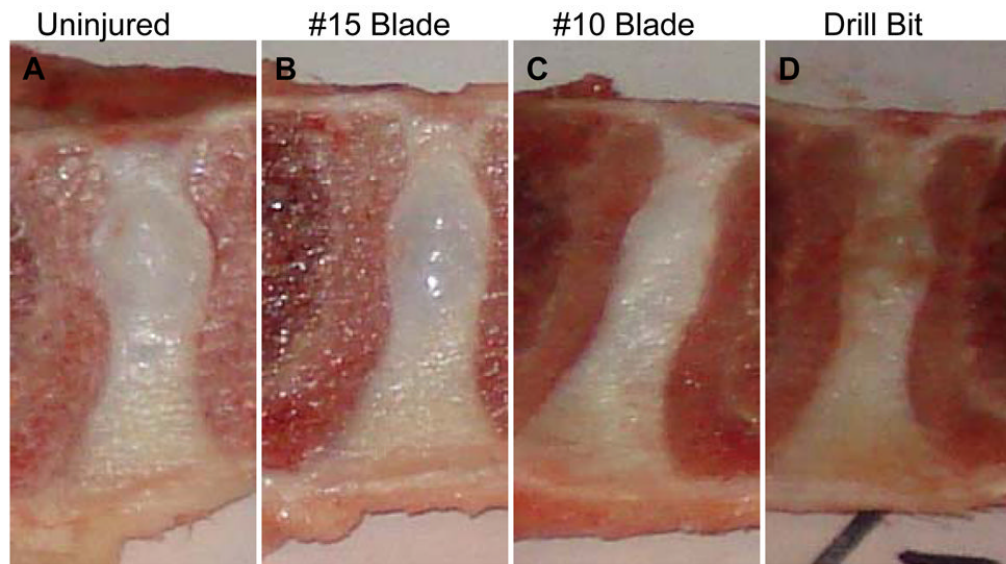


Figure 6. Photograph of gross sagittal sections of normal and injured intervertebral discs (IVD) with various instruments

A. uninjured disc; **B.** #15 blade cruciate injury; **C.** #10 blade inserted parallel to the endplate; and **D.** 4.5 mm diameter drill bit.

Table 1

Numerical histological scale for goat intervertebral disc (IVD) degeneration.

Score	0	1	2
*AF and NP Border	normal	minimal interruption	loss of distinction
AF organization	normal	slight disorganization	loss of organization
NP extracellular matrix	normal	mild condensation	Severe condensation
NP cellularity	normal	mild cell density change	profound cell density change

* AF = anulus fibrosus; NP = nucleus pulposus

Table 2

Histological grade two months after injury.

Total Histological Score	Uninjured (control)	#15 blade	#10 blade	4.5 mm drill bit
<i>Mean</i>	2.0	1.8	3.1	5.1
<i>Standard error</i>	0.46	0.62	0.79	0.65
<i>p-value (compared with uninjured control)</i>	N/A	0.1657	0.0783	0.0003

Table 3

Histological Score by Category.

Histological Score	AF and NP Border		AF organization		NP matrix		NP cellularity	
	uninjured	drill bit	uninjured	drill bit	uninjured	drill bit	uninjured	drill bit
<i>mean</i>	0.8	2.0	0.9	2.3	1.0	2.6	1.0	2.0
<i>Standard error</i>	0.12	0.23	0.12	0.20	0.12	0.15	0.12	0.23
<i>p-value</i>	0.0185		0.0048		0.0067		0.0086	